*Subcontractor Report*

# Process Development for CIGS-Based Thin-Film Photovoltaic Modules

## Phase I Technical Report
## 5 February 1998—4 February 1999

J. Britt, S. Wiedeman, R. Wendt, and S. Albright
*Global Solar Energy, L.L.C.*
*Tucson, Arizona*

**NREL**

**National Renewable Energy Laboratory**

# Process Development for CIGS-Based Thin-Film Photovoltaic Modules

## Phase I Technical Report
## 5 February 1998—4 February 1999

J. Britt, S. Wiedeman, R. Wendt, and S. Albright
*Global Solar Energy, L.L.C.*
*Tucson, Arizona*

**NREL**

**National Renewable Energy Laboratory**

**NOTICE**

Printed on paper containing at least 50% wastepaper, including 20% postconsumer waste

# Table of Contents

# List of Figures

# List of Tables

# Abstract

As a technology partner with NREL, Global Solar Energy (GSE) has initiated an extensive and systematic plan to accelerate the commercialization of thin film photovoltaics (PV) based on Copper Indium Gallium Diselenide (CIGS). GSE is developing the technology to deposit and monolithically integrate CIGS photovoltaics on a flexible substrate. CIGS deposited on flexible substrates can be fabricated into either flexible or rigid modules. Low cost rigid PV panels for remote power, bulk/utility, telecommunication, and rooftop applications will be produced by affixing the flexible CIGS to an inexpensive rigid panel by lamination or adhesive.

In the GSE approach, long (up to 700 m) continuous rolls of substrate are processed as opposed to individual small glass plates. Not until final module buss and power lead attachment is the continuous roll sectioned into individual panels. Roll-to-roll vacuum deposition has several advantages that translate directly to reduced capital costs, greater productivity, improved yield, greater reliability, lower maintenance, and a larger volume of PV.

In combination with roll-to-roll processing, GSE is developing evaporation deposition operations that enable low-cost and high-efficiency CIGS modules. In-line multi-source evaporation has been demonstrated at GSE to deposit high-quality CIGS films in a continuous roll-to-roll operation. Multi-source evaporation has other advantages including direct absorber formation (no selenization heat treatment) and high materials utilization of low-cost feed stock.

A two-pronged effort is underway to transition the CIGS deposition process into manufacturing at GSE. Effusion source development is conducted to improve the deposition uniformity and source robustness through design changes using a 16.5-cm web coater as a test platform. Successful modifications are incorporated into the design of effusion sources for use in a 33-cm manufacturing-scale web coater. As a result of this effort, a set of effusion sources is now installed in the 33-cm web coater that can provide excellent compositional uniformity across the web.

CIGS process development is focused on synchronizing the operation of the effusion sources, the Se delivery profile, substrate temperature, and a host of other parameters. A new GSE record cell efficiency near 10% has been achieved in the course of this process development. An program to substitute a stainless steel foil substrate for polyimide was initiated. A stainless steel product was selected and CIGS deposition optimization is proceeding. In the early stage of this effort, a roll-to-roll CIGS film on stainless steel was fabricated into a device with efficiency 8.4%.

Cell interconnection for thin film CIGS modules on a polyimide substrate presents a considerable challenge. An interconnect scheme has been selected and the equipment necessary to implement this scheme has been procured, installed, and tested. The scheme requires both an ink-jet deposition step and the removal of material by selective laser scribing. Process development is advancing rapidly and significant progress has been made. Continuous, ink-jet lines less than 200μm in width have been demonstrated. The integrity of laser scribes has been verified optically and electrically.

A primary objective of the GSE lamination program is to begin development of viable encapsulation and finishing methods to produce flexible and rigid mounted PV products. Initial GSE product lines have been defined and several of these initial designs have been demonstrated. Methods for high-throughput lamination have been incorporated into the GSE process. In particular, a four-minute EVA cure is under evaluation. The resulting costs of lamination for a given throughput are projected to be significantly lower than traditional methods utilized in the PV industry. Lead termination techniques have been incorporated, and are expected to provide high-performance, automate-able choices as next-generation development occurs. The primary focus in the next phase of this subcontract will be a multitude of product stressing and certifications. These product certifications are expected to include flexible, semi-flexible, and rigid module products.

**INTRODUCTION**

Thin film photovoltaic (PV) modules are the next evolutionary step towards cost-effective generation of electricity from sunlight. Thin film Copper Indium Gallium DiSelenide (CIGS) has been established as a leading contender to achieve that goal. Global Solar Energy (GSE) was founded to capitalize on the natural advantages of CIGS and develop a cost-efficient manufacturing scheme to bring the technology to market in a user-friendly form. The heart of the manufacturing scheme is all roll-to-roll vacuum processing on a continuous flexible polyimide substrate.

There are numerous challenges in developing the technology for manufacturing flexible CIGS photovoltaic modules. Three major areas deemed exceptionally challenging were selected by GSE for focused development under the Thin Film Partnership Program: 1) CIGS absorber improvement, 2) monolithic integration, and 3) encapsulation. The deposition of CIGS films on a continuous web by multi-source evaporation had never been attempted by any group before GSE undertook it and many unique difficulties must be confronted. Most conventional techniques for monolithic integration of thin film PV devices on glass substrates cannot be applied to integrate devices on a polyimide substrate. Novel interconnect schemes and processes must be developed. The encapsulation of a flexible module also presents special problems to solve, and unique advantages to employ.

The primary issues that are being addressed to improve the CIGS absorber are control of the effusion sources and development of processes that yield high-quality CIGS thin films. In particular, scaling up the source design for multi-source coevaporation over large areas (33-cm x 300-meter rolls of substrate) with adequate uniformity is an important goal. A great deal of effort has been focused on the design of the effusion sources. After numerous iterations, a complete set of effusion sources was successfully demonstrated in the CIGS manufacturing system during Phase I.

Another significant accomplishment that occurred during Phase I was the demonstration of a 9.8% device from CIGS deposited on polyimide in a roll-coater. The compatibility of GSE processes for CdS and the TCO depositions was continuously verified as improvements in the absorber deposition process were made. In addition, the groundwork for further efficiency increases was laid by initiating a program to incorporate Na into roll-coated CIGS films.

The advantages of depositing CIGS films on a stainless steel substrate were also recognized, and a program to explore roll-to-roll deposition on stainless steel was initiated. A preliminary result was the demonstration of an 8.4% efficient device from CIGS roll-coated onto a stainless steel substrate.

The many unknowns of integrating devices on a polyimide substrate have made the planned interconnect scheme (and equipment design) a calculated gamble. Significant delays were encountered in acquiring the equipment required for monolithic integration, but rapid progress in process development was made once the equipment was facilitated

at GSE.  Many aspects of the back contact, via, and front contact scribes have been verified by electrical and microscopic techniques.  The ink dispense technology, an integral part of the interconnect scheme, has demonstrated continuous ink lines less than 200 μm wide, comparable to good screen-printing, but with a much better registration accuracy.

Equipment to accomplish rapid lamination throughput of product at low costs for all initially envisioned product lines was identified and procured.  Two laminators are now installed, mostly debugged, and fully operational.  Materials and module layouts for planned products were also resolved and demonstrations of laminated active modules were accomplished at the GSE facility.  First-generation methods for lead termination (buss bar to lead connection) were identified, demonstrated, and are now incorporated into the "standard" process.  A conceptual design for a "buss bar and lay-up apparatus" was completed and that equipment, once incorporated, is expected to result in significant increases in productivity and quality in manufacturing.  GSE has also recently purchased a high-speed double bag laminator, and expects to take delivery early in Phase II.  The system was designed to laminate two 33 x 120-cm modules with a total cycle time of less than 10 minutes.

# 1.0  CIGS ABSORBER IMPROVEMENT


GSE has demonstrated a manufacturable roll-to-roll process for CIGS deposition on a 16.5-cm wide substrate by multi-source evaporation using an efficient source design. The overall objectives of this task are to improve the electronic quality of the absorber material and to refine and scale up the source design for multi-source evaporation over large area (33-cm x 300-m rolls of substrate) with adequate uniformity.  Control and reproducibility are critical issues continually addressed in the course of this work.

## 1.1 Deposition Process Optimization

Deposition parameters are adjusted for the CIGS layer to obtain sequentially higher electronic material quality.  A 16.5-cm roll coater is utilized as a test platform for the CIGS deposition process.  Improvements made to the deposition process in the 16.5-cm roll coater are translated and implemented in the manufacturing system.  The manufacturing system utilizes 33-cm wide web and differs from the 16.5-cm roll coater primarily in the sophistication of its components.  Deposition parameters that are varied for optimization include substrate temperature profile, selenium delivery profile, coating thickness, and final elemental composition.

CIGS grain size and morphology are critical guides to process development at GSE.  The upper working temperature of the polyimide, about 450°C, generally leads to submicron grains.  At this level, grain size is believed to have a strong influence on electronic material quality.  Grain size has been observed to depend strongly on CIGS film thickness, particularly for films less than 2.0μm.  In general, a balance must be struck between coating thickness and adhesion, as the two qualities are negatively correlated on flexible substrates.  In one deposition experiment, a range of coating thicknesses was obtained in a single deposition by simply by varying the web speed and hence the dwell time in the deposition zone.  The apparent CIGS grain size increased with the film thickness (Figure 1.1).  Similar observations have been made about CIGS deposited on glass substrates.



1.25 μm                                                    2.0 μm
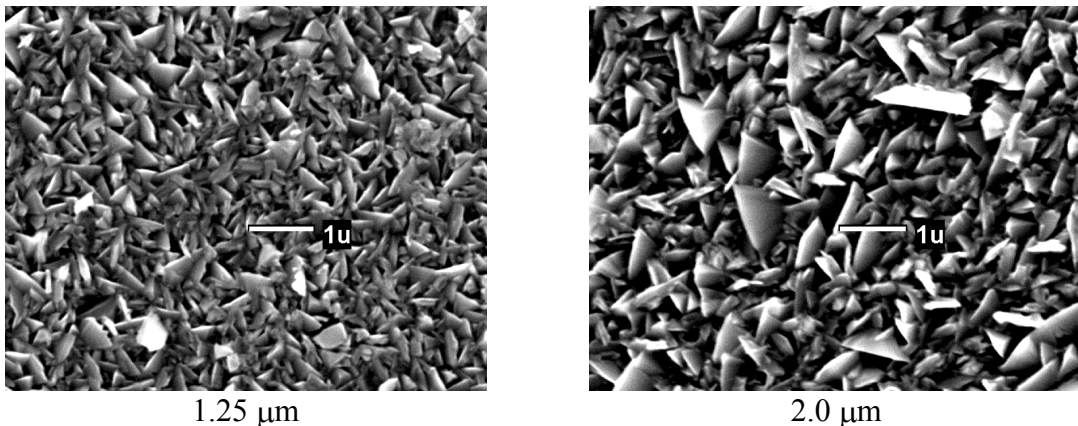
**Figure 1.1.**  SEMs of CIGS films deposited during a single deposition on polyimide/Mo with thicknesses 1.25 and 2.0 μm.

The film morphology is also significantly affected by the elemental composition. The surfaces of two CIGS films of different composition are shown in Figure 1.2. The films were deposited sequentially during a single run by varying effusion source temperatures. The more Cu-poor sample (Cu/(Ga+In) = 0.78) has finer grains and the surface is decorated with In-rich features not present on the other sample.



| Cu/(Ga+In) = 0.78 | Cu/(Ga+In) = 0.94 |
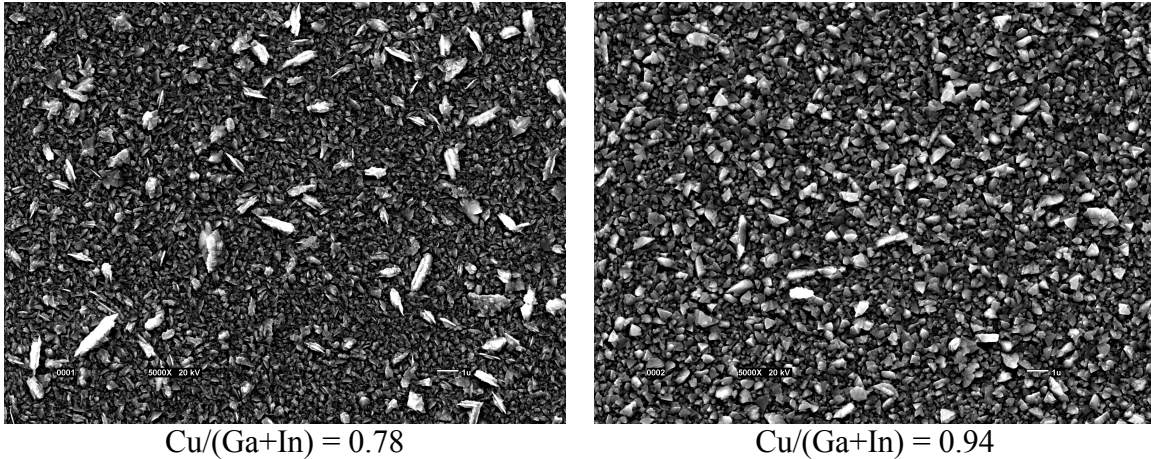
**Figure 1.2.** The effect of elemental composition on the morphology of CIGS films.

## 1.2 Source Scale-up

Effusion sources for multi-source evaporation must be mechanically and electrically robust and allow tight flux rate control and spatial uniformity over the substrate width. In addition, the sources must be very efficient to eliminate heat load on the substrate and system parts. Scaled-up effusion sources for deposition on 33-cm substrate widths (for roll coating 33-cm x 300-meter of substrate) have been designed, fabricated, tested, and implemented based on existing proven designs used in the 15-cm roll-coater. Effusion profile and rate modeling done in collaboration with the Institute of Energy Conversion (IEC), University of Delaware as a subcontractor have aided this effort.

### 1.2.1 Effusion Profile and Rate Modeling

A mathematical model developed at the Institute of Energy Conversion describes the evaporated flux from high rate effusion sources utilized by GSE. The model has been incorporated into an interactive Excel spreadsheet that allows a number of source parameters to be independently varied. The results are quantified and graphed to allow easy visualization. Among the user adjustable parameters are: deposition zone size, web speed and width, web to source distance, single source geometry and pool temperature, pool surface area, number and contents (Cu, Ga, In) of effusion sources, the spatial relationship between effusion sources, and chamber pressure. The output of the model provides instantaneous and cumulative composition (Cu/(Ga+In), Ga/(Ga+In)) at all points within the deposition zone as well as the terminal film composition and thickness.

An example of part of the spreadsheet output from the model is shown in Figure 1.3 for a source ordering Ga, Cu, In. The source ordering is relative to a fixed point on the web as it travels from the beginning to the end of the deposition zone. The normalized distance spans the length of the deposition zone. The terminal Cu/(Ga+In) and Ga/(Ga+In) in this example are 0.89 and 0.32, respectively.
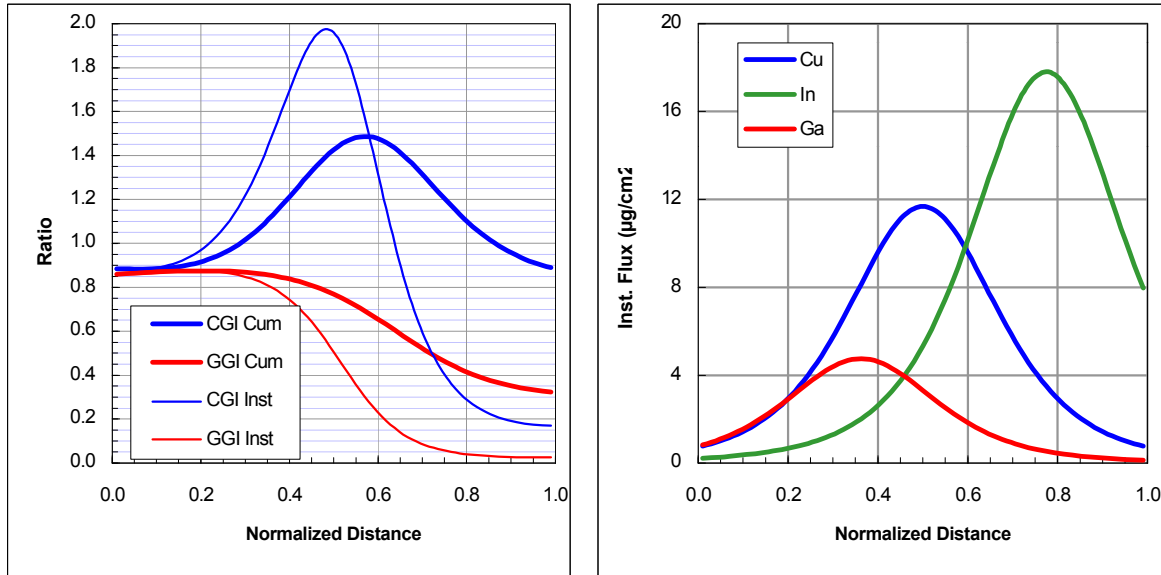


**Figure 1.3.** Graphical output from the effusion source model for the source ordering Ga, Cu, In.


### 1.2.2   Effusion Source Design and Construction

Careful design and selection of materials are necessary for constructing well-behaved effusion sources. The Cu source in particular demands great attention to detail as it is required to operate at temperatures greater than 1500°C in the presence of Se for long periods of time. The list of materials capable of sustained functioning in this environment is short. Successful source designs must account for thermal conductivity and expansion of all critical parts.

There has been much iteration in the source design at GSE. Some of the problems encountered are: heater element failure, deposition material build-up leading to source failure, excessive heat load to the web, and non-uniform effusion characteristics. Many of these problems are inter-related and solution of one problem exacerbates another. Still, an adequate understanding of these issues has been gained and successful source designs have been implemented.

### 1.2.3  Effusion Characteristics

The currently optimum design and operation of the effusion sources in the 33-cm yields CIGS films with good uniformity in composition across the width of the web (Figures 1.4 and 1.5).  The uniformity of CIGS thickness across the web can be improved (Figure 1.6), but should not be detrimental to module performance provided the minimum CIGS thickness is greater than about 1.8µm.
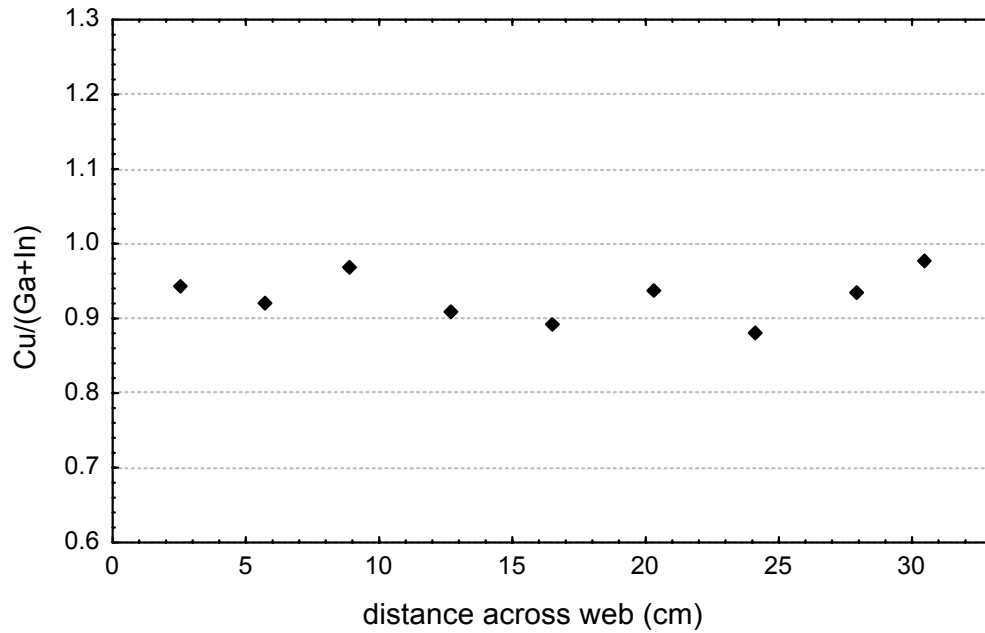


**Figure 1.4.**  CIGS composition variation (Cu/(Ga+In) across a 33-cm wide web.
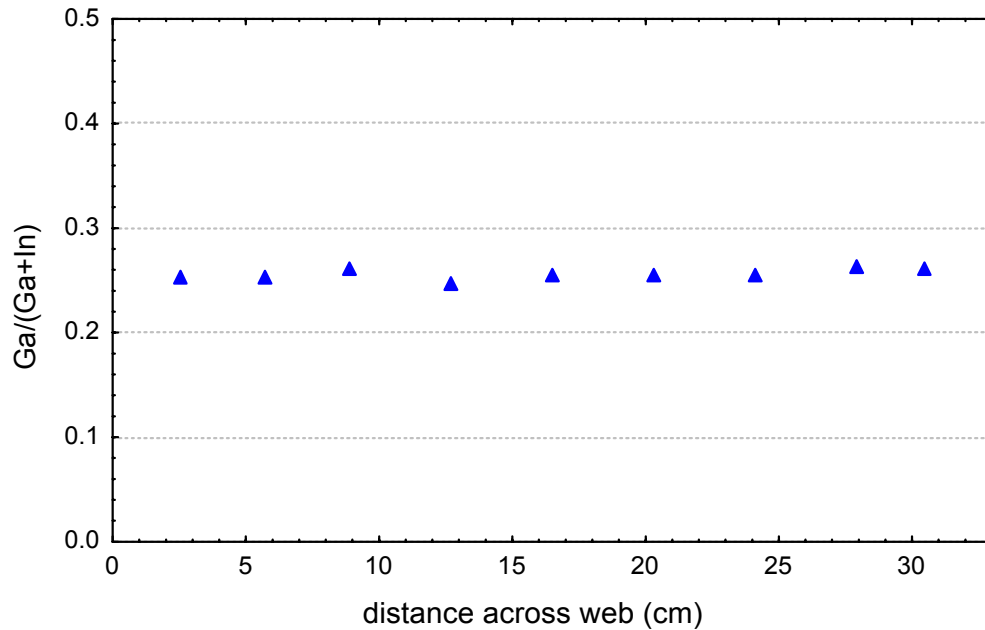


**Figure 1.5.**  CIGS composition variation (Ga/(Ga+In) across a 33-cm wide web.
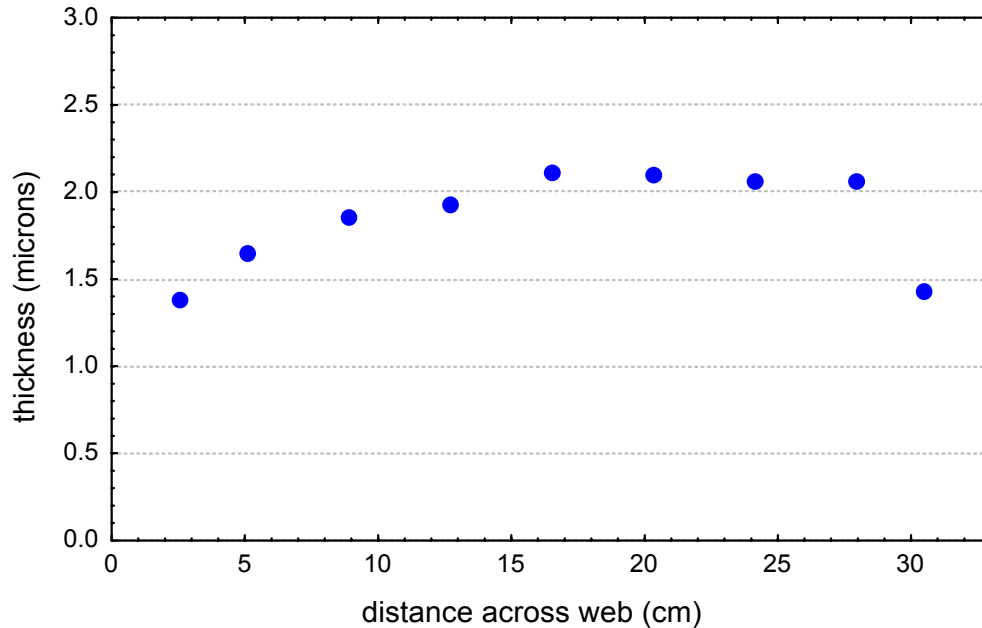
**Figure 1.6.** CIGS thickness variation across a 33-cm wide web.

## 1.3 Efficiency Improvement Studies

The goal of this effort is to attain sequentially higher small-area device efficiencies from CIGS deposited on 16.5-cm web and apply the knowledge gained to deposition on a 33-cm web. After meeting minimum device efficiency and uniformity criteria on the 33-cm web, optimization will be shifted to the submodule level. Improvements in efficiency are expected to result in part from optimizing the incident flux intensity profile at the substrate. The number and sequence of Cu, Ga, and In sources will determine the profile. Through subcontract, the Institute of Energy Conversion at the University of Delaware shares responsibility for materials and device characterization to facilitate efficiency improvement.

An investigation of sodium doping was also initiated during Phase I because of strong evidence from other groups that efficiency gains could result. Na is to be added extrinsically prior or during the CIGS film growth to enhance grain growth, carrier concentration, and ultimately the electronic quality of the absorber layer. The addition of Na is currently being effected by direct evaporation of a sodium compound. The investigation of Na doping is being conducted jointly with IEC under subcontract.

## 1.3.1    Effusion Source Sequence

The parameter space of the CIGS deposition process is large and would require considerable effort to explore exhaustively. One of the more closely examined parameters is the incident flux intensity profile at the substrate. The effusion model

developed at IEC (Section 1.2.1) has aided understanding of the effect of source arrangement on film composition in the GSE reactors.

Multiple effusion sources are used to deposit CIGS in the GSE reactors. The flux profile seen at a particular location on the web is determined by the arrangement of Cu, Ga, and In sources and their placement relative to one another. We have observed that the source arrangement and order can have profound effects on CIGS composition, adhesion, film density, and morphology.

A simple example is the effect of sequential source arrangements of In, Ga, Cu and Ga, In, Cu on the ratio Ga/(Ga+In). CIGS films with similar stoichiometry were deposited with these particular source sequences and the ratios Ga/(Ga+In) through the film thickness were calculated from SIMS profiles (Figure 1.7). The profiles reflect the source ordering. Apparently, Ga and In do not substantially interdiffuse under these deposition conditions. The lesson is that specific source arrangements must be utilized to achieve a desired composition profile.
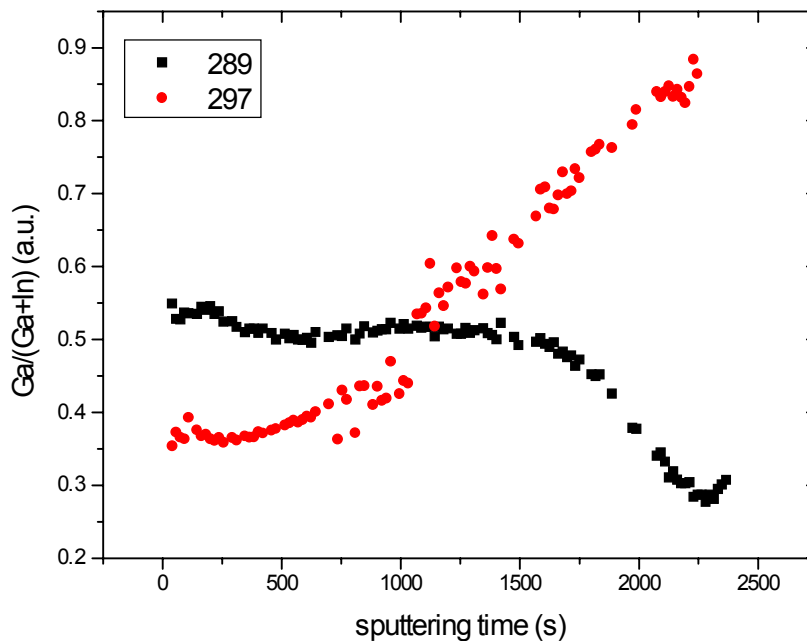


**Figure 1.7.** Ga/(Ga+In) as measured by SIMS for two source arrangements: 1) In, Ga, Cu (289), and 2) Ga, In, Cu (297) (A. Rockett, U. of Ill.).

An optimized source arrangement has been derived after a number of trials. The evaluation process was most heavily weighted by device efficiency. The ratios Cu/(Ga+In) and Ga/(Ga+In) for a typical CIGS film deposited under the standard conditions are shown in Figure 1.8. The ratios were calculated from Auger depth profiles.
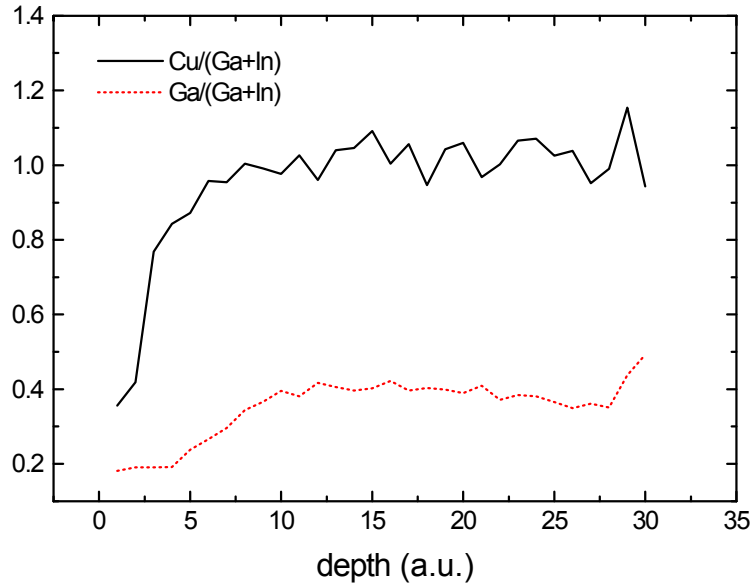
**Figure 1.8.** Cu/(Ga+In) and Ga/(Ga+In) depth profiles of a CIGS film deposited on polyimide using the standard source number and sequence (A. Swartzlander, NREL).

A GSE record cell efficiency of 9.8% was generated using the optimized source configuration (Figure 1.9). The structure of the device was polyimide/Mo/CIGS/CdS/i-ZnO/c-ZnO. CdS and ZnO films were deposited at IEC using their standard conditions; all other films were deposited at GSE. The J-V parameters for the 0.31-cm$^2$ device were measured at the IEC on a total area basis.



Cell 003
Voc = 0.487 V
Jsc = 30.6 mA/cm2
FF= 66.2 %
Eff = 9.8 %
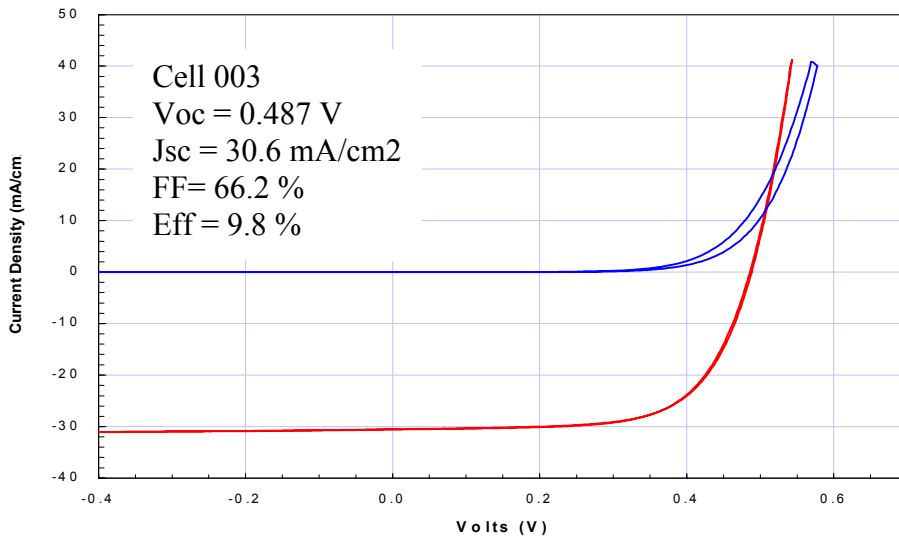
**Figure 1.9.** Light and dark J-V characteristic of a 9.8% efficient CIGS device deposited on Mo/polyimide.

### 1.3.2 Na doping of CIGS Films

CIGS films deposited on soda-lime glass receive a significant amount of Na by diffusion. Na has a significant effect on film morphology and electronic properties, such as carrier concentration. Literature data indicates Na can be added extrinsically in a controlled fashion to both improve device performance and consistency. Desirable properties of a process suitable for manufacturing are:

- Na deposition is not coincident with but <u>precedes</u> CIGS deposition for the sake of simplicity
- Na incorporation is efficient
- The Na compound has few impurities, and evaporates congruently or source evolution is limited in degree so as to limit Na poisoning in the system

Studies to investigate the extrinsic doping of CIGS with Na were initiated during Phase I. A list of potentially suitable compounds for the doping experiments was made (Table 1.1) and the most promising were procured.

**Table 1.1.** Properties of Na compounds.

| Compound | Mol. Wt. | m.p. (°C) | density (g/cc) | Comments |
|---|---|---|---|---|
| NaF | 41.99 | 993 | 2.558 | |
| NaCl | 58.44 | 801 | 2.165 | |
| NaBr | 102.89 | 747 | 3.203 | hygroscopic |
| NaI | 148.89 | 661 | 3.667 | hygroscopic |
| $Na_2S$ | 78.04 | 1180 | 1.856 | deliquescent |
| $Na_2Se$ | 124.94 | >875 | 2.625 | deliquescent, expensive |

NaI and NaBr were found to be so hygroscopic that the films fogged up within a few hours of being removed from the vacuum chamber. The $Na_2S$ source material itself contained a significant amount of water. After a long bakeout failed to eliminate all the water, $Na_2S$ was eliminated from further investigation. NaF did not appear to absorb water as quickly as the other compounds and subsequent work focussed on this material.

A series of trial doping experiments was made to investigate NaF further. One experiment consisted of evaporating 35Å, 75Å, 200Å, and 400Å of NaF on separate sections of a continuous polyimide/Mo web in a stationary mode. Thickness was monitored with a quartz crystal monitor. The web was rewound and CIGS was deposited on all sections during a single run. Material analyses and device fabrication was performed on the CIGS films deposited on evaporated NaF films.

Under the SEM, the CIGS grain size appeared unaffected when deposited on thinner (<200Å) NaF films and appeared to decrease on thicker NaF films (>200Å). A CIGS film deposited on a 75Å NaF film and its control with no extrinsic Na were analyzed by

SIMS.  The ratio Na/Se for the two films is plotted in Figure 1.10 as a function of depth through the films.  F in the films was found only near the detection limits of the SIMS measurement.  The rising "tail" at the back of both samples occurs at the Mo contact, presumably due to greater diffusion of Na than Se in Mo.  The high Na concentration near the surface of the control sample may be due to Na contamination after the CIGS deposition.  The Na level in the bulk of the extrinsically doped sample is about 30x greater than in the control sample.  This suggests that the attempt at incorporating Na throughout the film was successful.
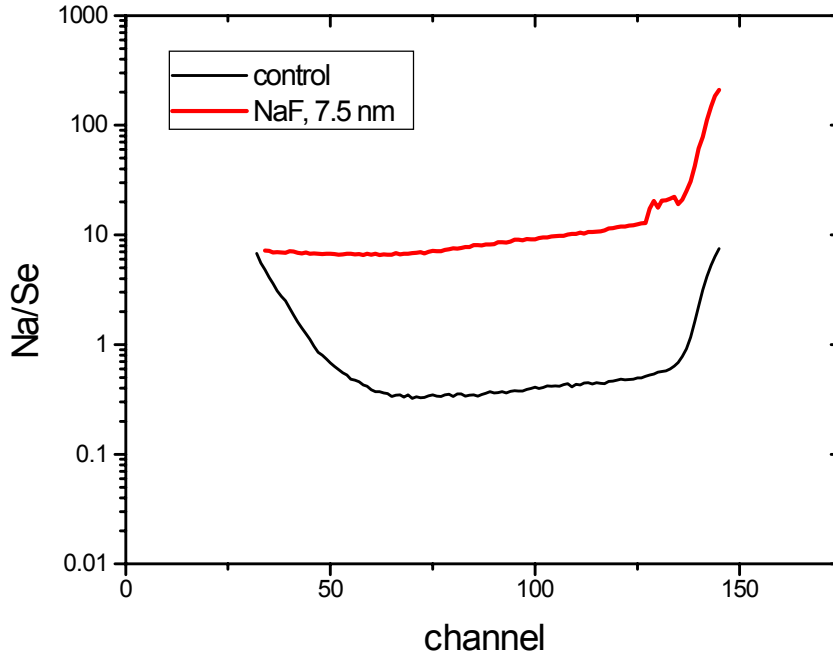


**Figure 1.10.**  Na/Se profiles of a NaF doped CIGS film and its control (A. Rockett, U. of Ill.).

A set of NaF doped devices was fabricated and characterized at IEC.  The device results were not encouraging (Table 1.2).  Looking at "best" cells from each set, there appears to be a substantial increase in $V_{oc}$, little or no change in fill factor, and a large decrease in $J_{sc}$ with increasing NaF thickness.  The net result is little or no change in efficiency.  The decrease in $J_{sc}$ may be attributed to the decrease in grain size of CIGS films deposited on NaF films over 75Å thick.  A potentially more significant problem is the decrease in yield with increasing NaF thickness.  The lower yield is due primarily to device shunting.

**Table 1.2.**  Device characteristics of NaF-doped CIGS films.

| NaF thickness (Å) | 0 | 35 | 75 | 200 |
|---|---|---|---|---|
| $J_{sc}$(mA/cm$^2$) | 29.5 | 28.1 | 29.4 | 23.8 |
| $V_{oc}$(Volts) | 0.449 | 0.444 | 0.470 | 0.541 |
| FF(%) | 58.0 | 56.2 | 54.7 | 60.2 |
| $P_{max}$(mW/cm$^2$) | 7.69 | 7.02 | 7.56 | 7.75 |

Future work will attempt to eliminate some of the problems already uncovered, particularly poor device yield. The means to evaporate Na compounds *in-situ* immediately prior to CIGS deposition has been implemented to circumvent the issue of hygroscopicity (and possibly poor yield). New buss bars, feedthroughs, shielding, copper cables, and a transformer have been installed in the 16.5-cm system, and a QCM/shutter/controller has been integrated to control the rate onto the moving web.

## 1.4 Heterojunction Formation Capability

A series of round robin experiments was conducted between IEC and GSE to identify and understand major differences between the existing baseline process (CBD CdS/i-ZnO/c-ZnO) and the final manufacturing process (vacuum-deposited CdS/TCO). IEC was responsible for depositing CBD CdS and ZnO and GSE for the manufacturing processes. Common CIGS deposited on polyimide at GSE was used for all the experiments. Contact grid deposition and characterization was done at IEC.

In a characteristic experiment, a common CIGS/Mo/polyimide sample had CdS deposited on one section by chemical bath deposition at IEC and CdS vacuum-deposited on another section at GSE. IEC deposited i-ZnO/c-ZnO and grids on both samples simultaneously. The device properties of cells from each type are listed in Table 1.3. A higher open-circuit voltage and fill factor in the sample with CBD CdS is partially offset by the larger $J_{sc}$ in the sample with vacuum-deposited CdS.

**Table 1.3.** Comparison of devices with CBD and vacuum-deposited CdS.

|  | Voc (V) | Jsc (mA/cm$^2$) | FF (%) | Eff. (%) |
|---|---|---|---|---|
| CBD CdS (IEC) | 0.465 | 25.8 | 64.0 | 7.68 |
| Vacuum-deposited CdS (GSE) | 0.443 | 27.0 | 62.7 | 7.50 |

Two other samples from GSE had CBD CdS deposited on them at IEC. One sample was returned to GSE and had standard TCO deposited on it. The other sample had i-ZnO/c-ZnO deposited on it at IEC. Both samples were characterized at IEC by JV (Table 1.4) and QE. The primary difference in JV performance is a 15% lower $J_{sc}$ for the sample with TCO deposited at GSE. At least some of the difference in $J_{sc}$ can be attributed to more free-carrier absorption in the GSE TCO. The normalized QE's indicate the presence of wavelength independent losses in the GSE sample.

**Table 1.4.** Comparison of devices with TCOs deposited at IEC and GSE.

|  | Voc (V) | Jsc (mA/cm$^2$) | FF (%) | Eff. (%) |
|---|---|---|---|---|
| i-ZnO/c-ZnO (IEC) | 0.478 | 31.2 | 63.6 | 9.47 |
| TCO (GSE) | 0.457 | 26.0 | 64.5 | 7.67 |

## 1.5 Stainless Steel Substrates

The deposition of CIGS on polyimide is effectively limited to temperatures below 450°C, the recommended maximum working temperature of the polyimide. Unfortunately, this constraint leads to less than optimal device efficiency. As an alternative to polyimide, GSE began an investigation of stainless steel foil substrates under the Thin Film Partnership Program late in Phase I. The investigation was prompted by the many desirable properties of stainless steel and the excellent efficiencies achieved on stainless steel by the CIS group at NREL. The research at GSE is simplified by the fact that stainless steel foil is a drop-in replacement for polyimide film in all the roll-to-roll thin film deposition processes.

Stainless steel foils are available in a variety of types, thicknesses, tempers, and finishes. A study of stainless steel properties was made prior to obtaining any foils for deposition experiments. The different types of stainless steel were compared for corrosion resistance (composition), thermal expansion coefficient, availability, and cost. Several foil samples were procured to evaluate surface finish by profilometry. Two types of stainless steel were then selected and procured in roll form for further evaluation.

Long sections of stainless steel were coated with a back contact and cut into smaller sections for coating with CIGS. Minor modifications were made to the 16.5-cm roll coater to account for the different material properties of stainless steel and polyimide. For instance, a new web heater assembly was installed in to take advantage of the higher processing temperatures allowed by stainless steel, up to 600°C. Several CIGS depositions were conducted in the short period of time remaining in Phase I. Most of the CIGS films were extrinsically doped with Na.

The apparent grain size of the CIGS films deposited on stainless steel was substantially larger than that of films deposited on polyimide in the same reactor at a lower substrate temperature (Figures 1.11 and 1.12). Several samples were also analyzed by Auger depth profiling at NREL. The Ga/(Ga+In) profiles of the CIGS films deposited on stainless steel at GSE (an example is shown in Figure 1.13) show far less influence from source arrangement than CIGS films deposited on polyimide at a lower substrate temperature. Presumably, this is due to enhanced diffusion at the higher substrate temperature.

Several CIGS samples were processed into devices at NREL and characterized (F. Hasoon). Device efficiencies as high as 8.4% were measured. The J-V characteristics of the best device were $V_{oc}= 0.472$ V, $J_{sc}= 29.2$ mA/cm$^2$, and fill factor 60.8%. Little process optimization was performed to achieve this result. Significant forward progress in roll coating CIGS on stainless steel foil is anticipated in the near future as more effort is applied.
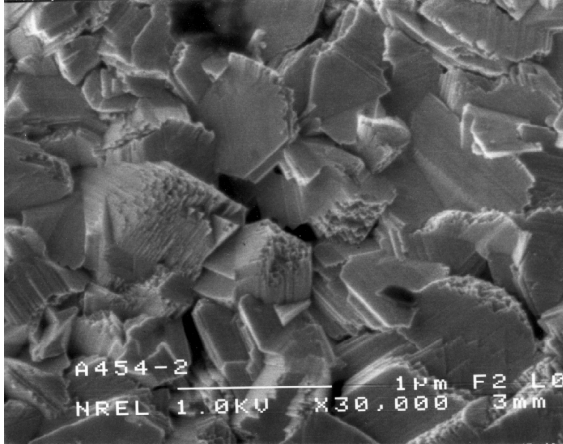
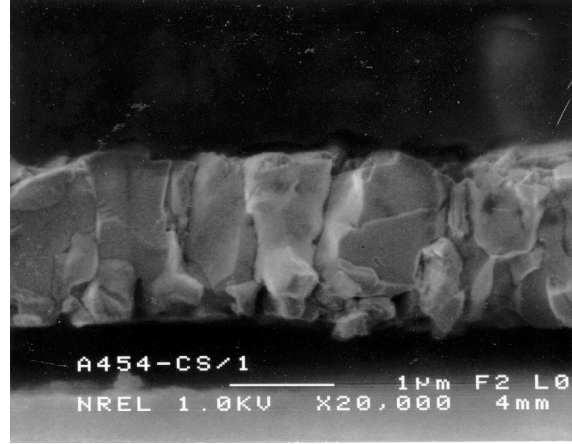**Figure 1.11.** Surface SEM of a CIGS film deposited on stainless steel (F. Hasoon, NREL).



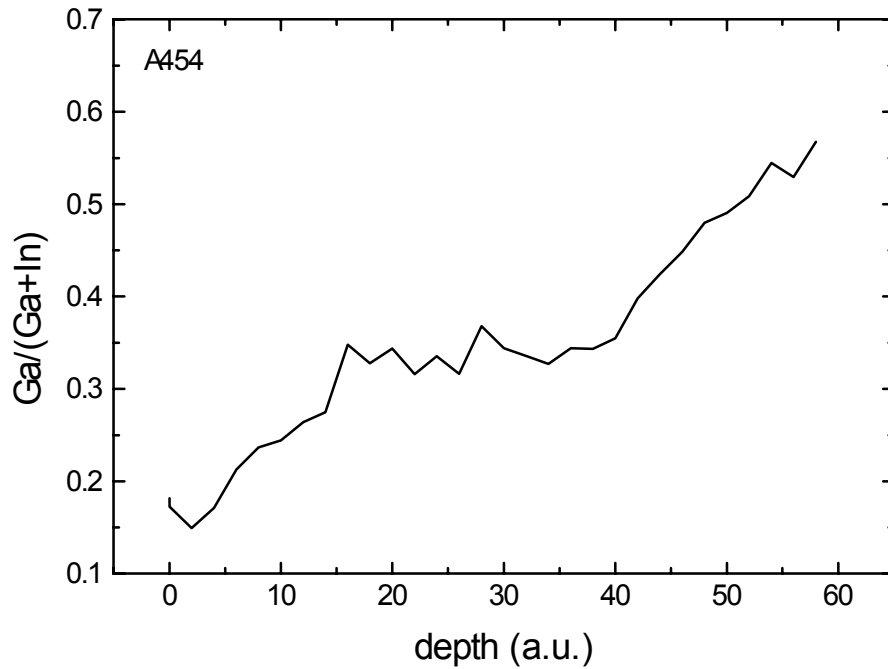**Figure 1.12.** Cross-section SEM of a CIGS film deposited on stainless steel (F. Hasoon, NREL).



**Figure 1.13.** Ga/(Ga+In) of a CIGS film deposited on stainless steel (A. Swartzlander, NREL).

## 2.0 MONOLITHIC PROCESSES FOR INTEGRATION OF LARGE AREA PV

The objective of monolithic integration at GSE is to develop low-loss scribe and interconnect processes for module formation on a flexible polyimide substrate. Our approach includes layer-specific, all-laser scribing methods, coupled with the development of ink-jet deposition of insulating material over scribes.

### 2.1 Layer-Specific Laser Scribing Processes

Several different methods can be used to form serial monolithic interconnections between module segments, as shown in Figure 2.1 below. In Figure 2.1 the sequence of operation is denoted by the physical layer deposited, or the scribe made (S1, S2, etc) or the insulating layer printed (P1, P2, etc.), and W denotes a 'weld' operation. Most of the effort to date at GSE has been toward implementation of an all-laser post absorber 3 method. The post absorber 3 method prevents the introduction of any scribing debris until after absorber layer deposition and requires fewer steps than the other post absorber methods or the post device method.

Equipment required to accomplish the monolithic integration on flexible substrates at GSE has been completed in Phase I. The scribing station at GSE has facilities for high speed movement and placement of the laser beam relative to the module with micron resolution. The scribing station also incorporates machine vision capabilities for fiducial recognition and scribe inspection, and facilities for transporting and holding continuous, flexible webs of PV material under process.
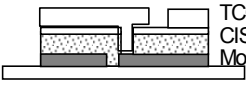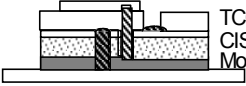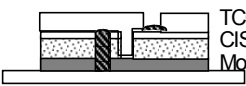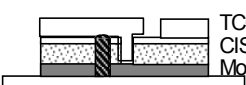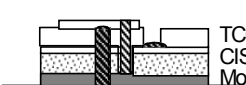
| Configuration | Interconnect Sequence | |
|---|---|---|
| Cascade | Mo/S1/CIS/CdS/S2/TCO/S3 | TCO CIS Mo |
| Post Absorber 1 | Mo/CIS/CdS/S1/P1/TCO/ P2/S2&W | TCO CIS Mo |
| Post Absorber 2 | Mo/CIS/CdS/S1/P1/TCO/S2 | TCO CIS Mo |
| Post Absorber 3 | Mo/CIS/CdS/S1/P1/TCO/S2 | TCO CIS Mo |
| Post Device (TCO) | Mo/CIS/CdS/TCO/S1/P1/ P2/S2&W | TCO CIS Mo |

**Figure 2.1.** Various methods considered to form module interconnects at GSE.

Provision has been made on the scribing station to deliver the laser beam for scribing operations. Rather than screen printing, ink jet methods were proposed, and have been developed to allow deposition of insulating material into the scribes. The proposal of ink jet methods over screen printing was motivated by the potential for finer linewidths and better registration accuracy, and flexible pattern generation. The ink jet deposition equipment is also incorporated into the GSE scribing station.

Several significant challenges exist in the post absorber 2 approach, one of which is the requirement for selective removal of specific layers. The first scribe must remove the CdS, CIGS and the Mo down to the polyimide substrate material without substantial damage to the polyimide. Similarly, for the the interconnect scribe the Mo back contact must be exposed, but left largely intact. Perhaps the most demanding is the front contact scribe, in which the thin layer of TCO must be selectively removed without significant damage to underlying layers. Presently, most organizations use mechanical scribing methods to accomplish the front contact scribe. Mechanical methods were avoided at GSE, however, because the flexible polyimide substrate is easily deformed and damaged by mechanical scribing.

Shown in Figures 2.2 and 2.3 below are scanning electron micrographs of back contact laser scribes. Notable features include fairly clean removal of the CdS, CIGS and Mo down to the polyimide.
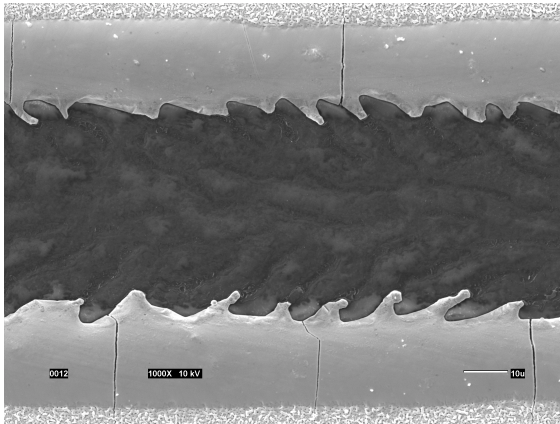


**Figure 2.2.** Top view micrograph of a back contact scribe made on a CdS/CIGS/Mo/polyimide stack.
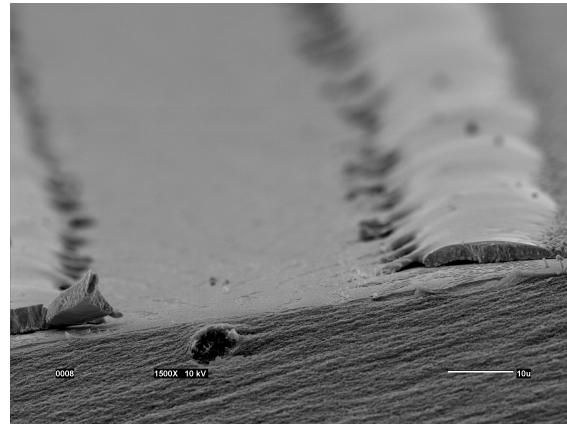


**Figure 2.3.** Perspective view of the back contact scribe shown in Figure 2.2. showing clean removal down to the polyimide substrate.

Under optimum conditions there is little damage to the polyimide substrate. As seen in Figure 2.3 a berm of material adjacent to the back contact scribe is typically formed, although this material is well adhered and there is little generation of loose debris. Electrical tests indicate that for back contact scribes made under the proper conditions the electrical isolation is adequate for monolithic integration.

The "via" or interconnect scribe also requires selective removal of material, similar to the back contact scribe, except that the back contact Mo layer must be left wholly or at least

substantially intact. Unlike the back (and front) contact scribes, the interconnect scribe need not be continuous. Shown in Figure 2.4 is a micrograph of an interconnect scribe made using laser processing at GSE. Scribe conditions can be selected that effect complete material removal in small 'islands' down to the polyimide through the Mo back contact. EDS analysis indicates that the back contact metal is well exposed in the border regions of the 'islands' visible in Figure 2.4, presumably allowing good electrical contact with the TCO that is subsequently deposited.
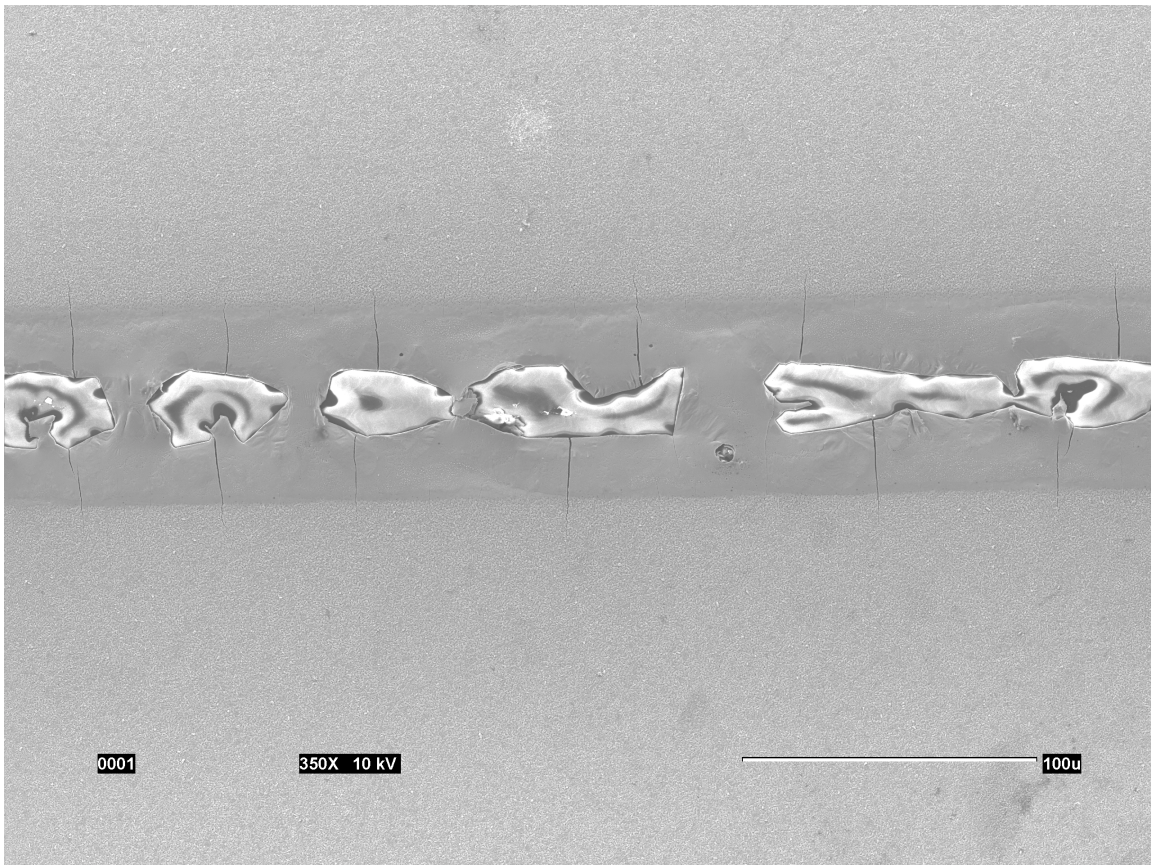


**Figure 2.4.** A top view micrograph of an interconnect scribe made on a CdS/CIGS/Mo/polyimide stack.

Interconnect test structures are utilized to optimize the via. The goal is to maximize the electrical conductivity from the front to the back contact through the interconnect scribe, and thus minimize the series resistance in the monolithic interconnection.

Front contact scribes have also been developed at GSE, again using all-laser processing. In Figure 2.5 a top contact scribe is visible in which the front contact material, in this example indium-tin oxide (ITO), has been selectively removed. Complete removal of the ITO is further supported by composition analysis taken by EDS on an area inside the scribe compared to that outside the scribe (see Table 2.1). The EDS analysis in Table 2.1 was done at 10 kV. Although using such low beam energy for EDS permits greater

surface sensitivity, it should be noted that analysis at such low energy does not yield accurate relative composition of elements such as Cu, Ga, Se and In because many important characteristic lines are not excited.

**Table 2.1**. Elemental composition by EDS at 10kV for typical areas inside and outside the scribe shown in figure 2.5. An asterisk denotes signal levels below statistical significance.

| Element | Outside Scribe | Inside Scribe |
|---------|----------------|---------------|
| Sulfur | 5.04 | 0.57 * |
| Selenium | 2.05 | 37.57 |
| Cadmium | 7.98 | 1.89 |
| Copper | - | 29.81 |
| Indium | 76.13 | 21.82 |
| Gallium | - | 4.90 |
| Tin | 6.85 | 0.45 * |

It is evident that EDS picks up predominantly a tin and indium signals outside the scribed region, with a little cadmium and sulfur signal from the underlying CdS. Inside the scribed region the ITO has been removed, indicated by the lack of a tin signal.



**Figure 2.5.** An SEM micrograph showing a top view of a front contact scribe made on a device stack of ITO/CdS/CIGS/Mo/polyimide.

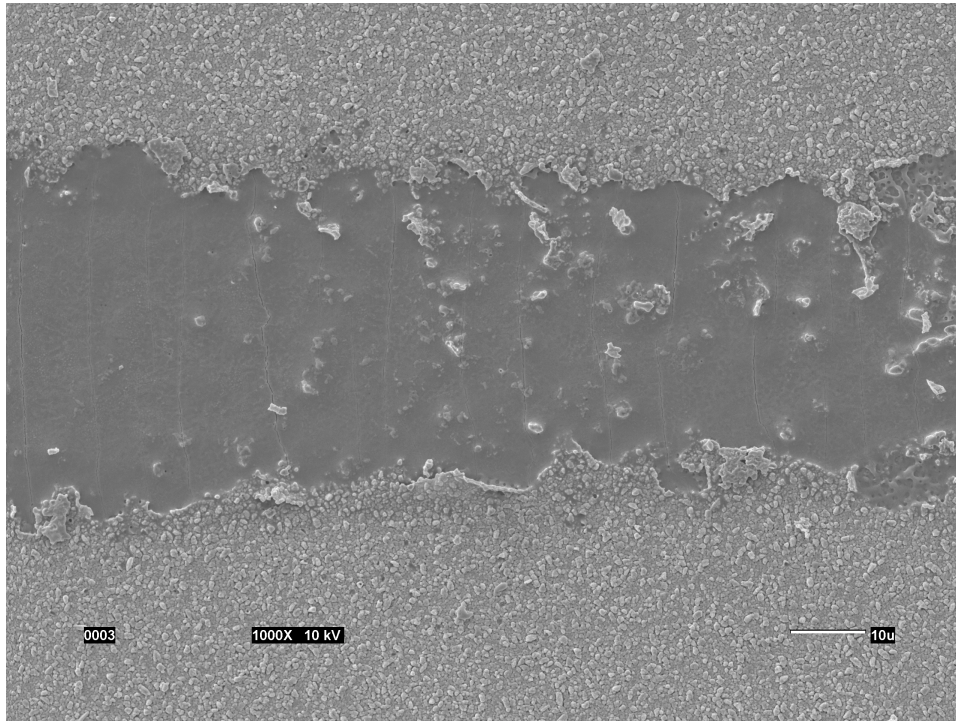Removal of the front contact TCO can be directly observed in perspective view micrographs shown in Figures 2.6 and 2.7. In those views, the fine structured material on

top appearing as a coating is the ITO. The edge of the scribed region shows removal of the ITO exposing the underlying CIGS layer. In Figure 2.7 the Mo back contact layer is also visible.



**Figure 2.6**. Micrograph of a front contact laser scribe on ITO/CdS/ CIGS/Mo/polyimide.

**Figure 2.7**. Higher magnification micrograph of front contact laser scribe showing selective removal of the ITO

## 2.2 Ink Dispense Technology for Module Integration

The post absorber and post device techniques for monolithic integration detailed in Figure 2.1 also require the deposition of a line of insulating material over one or more of the scribes. For the post absorber approaches, the deposited insulating material in the back contact scribe prevents direct shunt formation from the front to the back contact upon subsequent TCO deposition. Requirements for the insulating line of material are compatibility with the TCO deposition conditions, good adhesion, and high electrical resistance. The insulating line must be continuous and uniform. The insulating line width must also be minimized to avoid loss of active area on the module. As a result, the registration tolerance is decreased. GSE has is developing an ink-jet method to deposit the lines of insulating material over the scribes. The qualities of the deposited insulating line are dependent on many parameters, including fluid type, dispense pressure, and physical distances and speeds of the ink-jet dispenser relative to the substrate.

Significant progress has been made in the development of a viable technique for ink-jet deposition of insulating material for monolithic integration. Variation of important parameters has begun to optimize the ink-jet deposition process. An example of data taken for one type of insulating material is shown in Figure 2.8, showing the dependence of linewidth on dispense pressure.
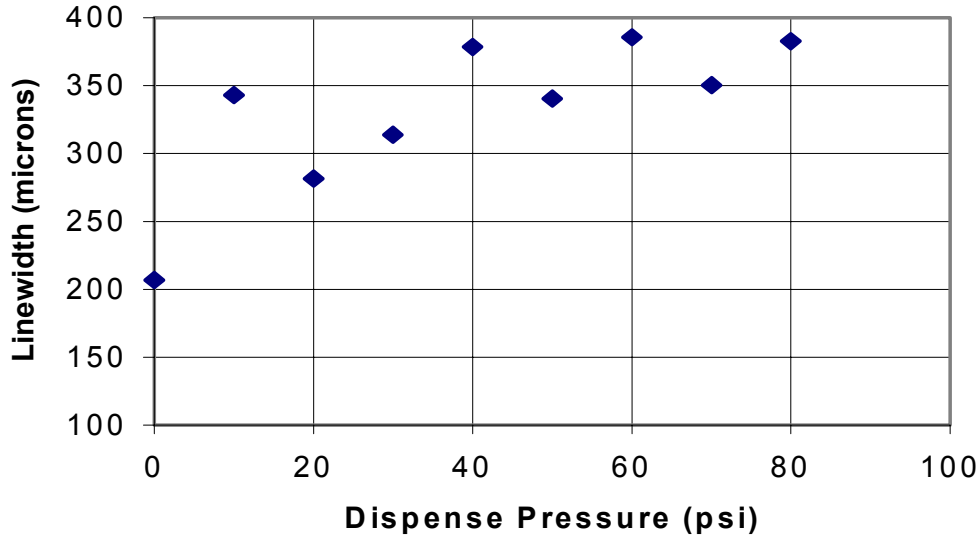
**Figure 2.8.** The dependence of linewidth on ink-jet dispense pressure for one type of fluid.

As a result of optimization to date, GSE has been able to significantly reduce the line width of the insulating material, and to improve the uniformity and control of the process. Shown in Figures 2.9 and 2.10 are examples of printed insulator lines using the ink-jet equipment at GSE. Due to process improvements, the line in Figure 2.10 is much more uniform and much thinner than that shown in Figure 2.9. The difference in linewidth is even greater than apparent from the micrographs, because the image in Figure 2.10 is taken at twice the magnification of Figure 2.9.

Although further development is required, significant progress has been made in developing the ink-jet deposition technology for use in PV module monolithic integration.
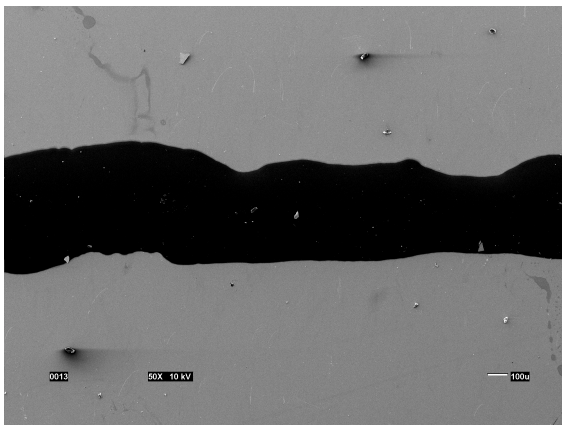


**Figure 2.9.** A micrograph of an early attempt at deposition of insulating material using the ink-jet approach.
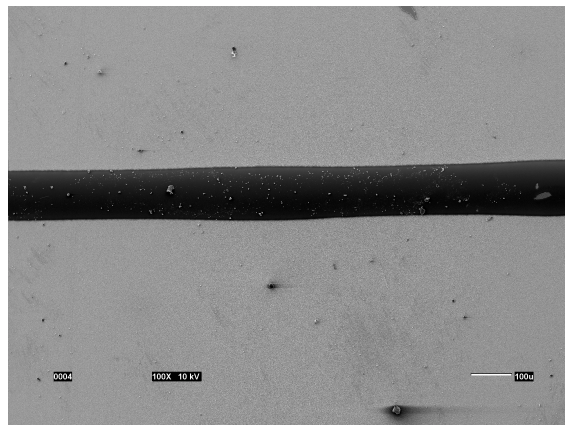


**Figure 2.10.** A micrograph of an insulating line printed by ink-jet means.

20

# 3.0  ENCAPSULATION DEVELOPMENT AND RELIABILITY TESTING

## 3.1 GSE Product Description

Two initial product lines with a third line added later are envisioned to meet the needs of the identified markets. Additionally, these three lines; the flexible, the semi-flexible, and the rigid designs are each ultimately expected to be certifiable by UL. The goals of this NREL subcontract have allowed focussed efforts to be applied to developing and demonstrating first generation product designs.

### 3.1.1  Market Considerations

One of the primary competitive advantages of the GSE technology is the ability to make whatever size and design of product necessary to meet market needs without complex or expensive re-tooling. This advantage comes from starting with a roll-to-roll deposition process that prepares a low-cost, high-performance lightweight, flexible, ready-to-encapsulate PV material.  Furthermore, it is clear that the ability to attach the flexible GSE substrate to a variety of module backings (including curved, flexible, and non-flexible materials) is much more feasible than for most other PV technologies.

In addition to the module wattage, an important design consideration/constraint for all modules is the desired voltage of the product. The desired maximum power point voltage ($V_{mp}$) requires a certain number of individual cells connected in series, and for maximum module efficiency there is an optimum cell width to be considered.  Whether flexible, semi-flexible, or rigid, the desired maximum power point voltage ($V_{mp}$) for the various products are predominantly ~16.5V and ~65V.  Some identified markets require ~33V and ~48V.
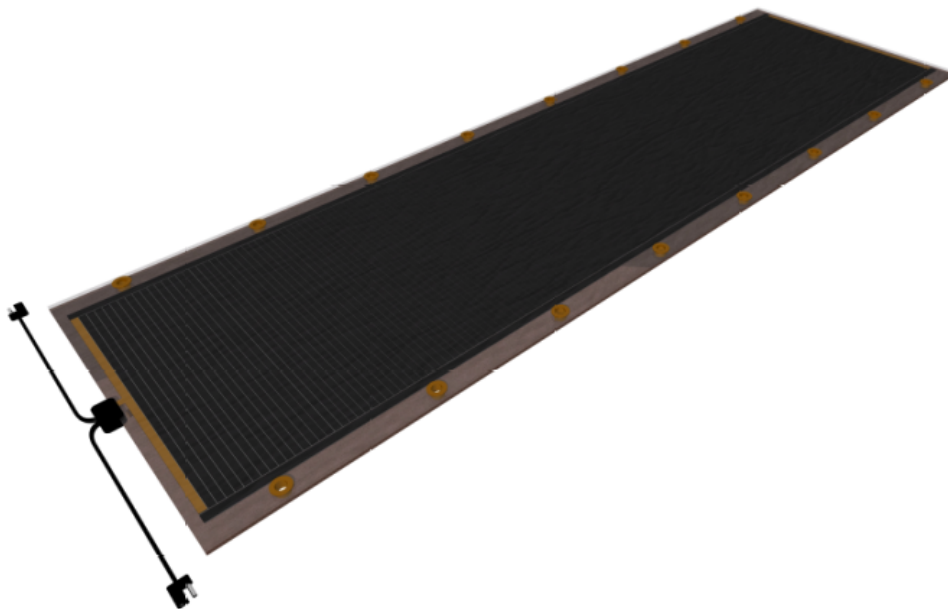


**Figure 3.1.**  120-cm long module design with ~160 series connected cells, 65$V_{mp}$ module.

The lowest cost module configuration results from monolithically cutting the web perpendicular to the web direction and cutting the web to the longest practical length. The resulting voltage from a 120-cm long module with ~160 monolithically interconnected strips is expected to result in a $V_{mp}$ of ~65V [See Figure 3.1]. Modules with a length of 90-cm are expected to meet the needs of markets that require a $V_{mp}$ of 48V. A second configuration utilizes ~31-cm long sections of web with ~40 series strips that result in a $V_{mp}$ of ~16.5V, for battery charging applications. These web sections are turned perpendicular to the module axis as shown in Figure 3.2 and interconnected as needed for ~16.5V and ~33V $V_{mp}$ markets.
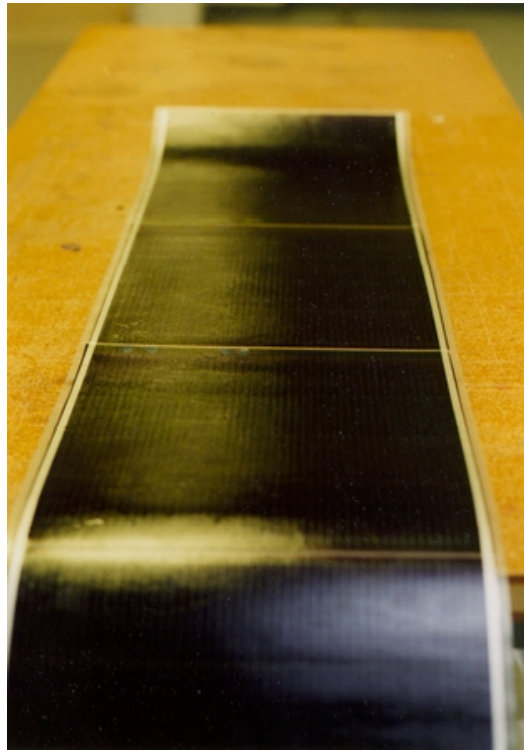


**Figure 3.2.** 120-cm long module design with ~40 series connected cells per section, 16.5V$_{mp}$ module.

Virtually any voltage required for achieving market access could easily be fabricated commercially for a given wattage due to the "flexibility" of the product. All three of product lines, flexible, semi-flexible, and rigid, are expected to be ultimately certifiable by UL, IEEE, and internationally. A general description of each of the three envisioned product lines follows:

### 3.1.2 Flexible Products

The module in this case [See Figure 3.3] is structured as Tefzel - EVA (Crane glass) – thin module – EVA (Crane glass) – Tri-laminate (or, in some product lines, Tefzel again). This module type [See Figure 3.1] is not envisioned to have a mounting frame at this time, although it can be easily attached to a variety of structures. The J-Box is a small, potted version with wire whips. Versatile in many markets, these unframed, flexible modules are envisioned to be either unmounted, mounted through grommets to a non-rigid or rigid structure (e.g. ground, tent,

strung-up to a structure, etc.), or mounted to a fixed structure with pop rivets, screws, tie-downs, etc. [See Figure 3.4]. Once potted, the inside of the J-Box is inaccessible. Therefore, in production, the wiring configuration coming out of the J-Box needs to be decided upon prior to completing, testing, and shipping the modules.



**Figure 3.3.** Flexible module lamination layers.
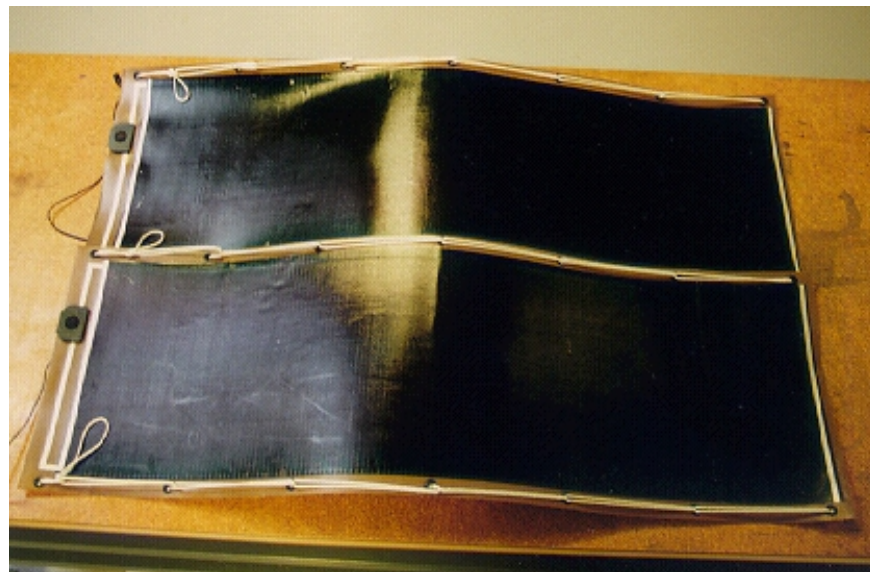


**Figure 3.4.** Flexible module with grommets for hold-downs.

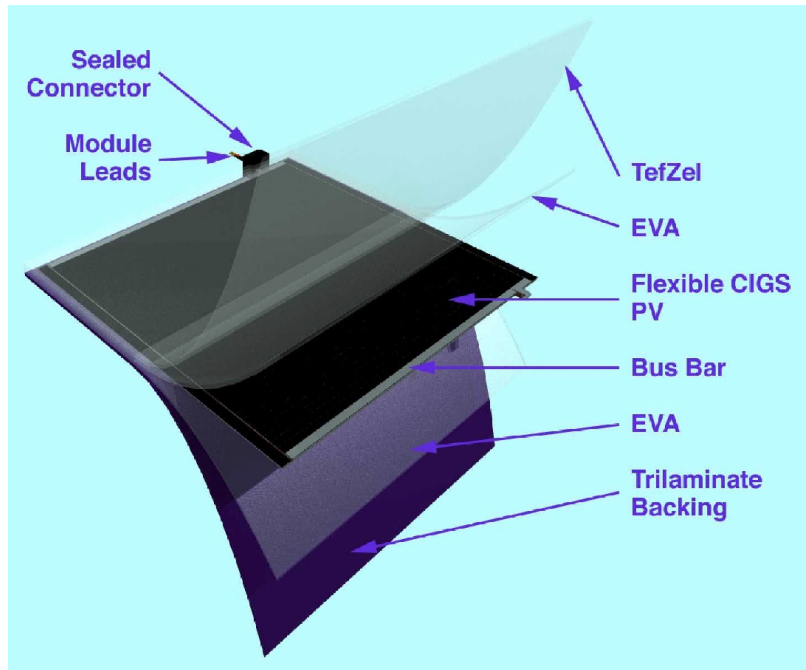Most of the envisioned products utilize mainstream PV materials for construction. This listing includes:

- Tefzel as a transparent, flexible, low-friction cover-layer,
- Ethylene Vinyl Acetate (EVA) as a proven lamination adhesive.
- In cases where the structure utilizes Tefzel, a Crane glass layer is included to provide additional needed resistance to cutting and piercing of the module.
- The Trilaminate backing material is presently chosen for many products due to its flexible, low-friction nature and its improved adhesion characteristics when used with EVA compared to a straight Tedlar backing.

Additionally, due to the "flexibility" of the product, a variety of alternative materials are expected to be utilized as a backing material in specialty markets including canvas, foils, and various plastics; rigid and flexible, planar and curved.

### 3.1.3 Semi-Flexible Products

The module in this case is structured as Tefzel - EVA (Crane) - thin module – EVA – anodized aluminum sheet (0.030-in thick). This module is to have a mainstream design for a mounting frame and a mainstream design for a J-Box. The aluminum mounting frame is grounded to the aluminum sheet. Due to accessibility, the J-Box can be configured in all possible wiring configurations in the field rather than in the manufacturing facility. A photo of such a module (unframed in this case) is shown in Figure 3.5.



**Figure 3.5.** Semi-flexible module.

### 3.1.4 Rigid Products

The third case is used for applications that require a traditional structure. This third product line will also be developed in the intermediate future. It has a structure of glass - EVA – thin module – EVA – glass. Materials costs for the module alone are actually lower for this version than for other designs. It must be noted however, that overall installed costs of the flexible and semi-flexible modules turn out to be lower in most applications due to the lower costs of framing, packaging, handling, shipping, and mounting that are not achievable with glass-based module designs.

The "flexibility" of the monolithically interconnected web of GSE's CIGS-based material clearly enhances the competitive advantages of GSE by enabling GSE to rapidly access new market that are not available to other technologies.

## 3.2    High Speed Lamination of Flexible Substrate to Flexible Backing

The objective of this subtask is to design, fabricate, install, and test lamination equipment capable of low-cost lamination of solar panels that meet initial throughput, economic, and market needs of GSE. A throughput rate of 1-ft$^2$ per minute has been utilized as the initial goal for a lamination building block for expansion of manufacturing. This section describes the primary accomplishments against the objectives within this subtask.

Material selection for the flexible module designs was discussed in the Section 3.1. The critical material for lamination is Ethylene Vinyl Acetate (EVA), a thermosetting thermoplastic used religiously within the photovoltaic field. The time and temperature profile required for the properly curing the EVA is well proscribed by the suppliers. During this contract it was recognized that the addition of Crane glass to the EVA was necessary to pass the IEEE and UL "Cut Test".
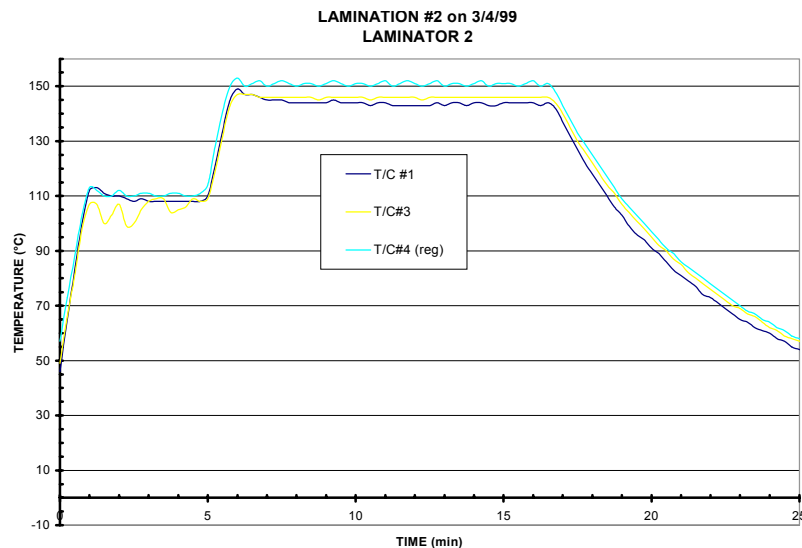


**Figure 3.6.** Time-temperature profile utilized in the laminators to cure EVA.

A conceptual design for curing Ethylene Vinyl Acetate (EVA) laminates via a single bag laminator was identified prior to this subcontract. During this subcontract, this high-throughput laminator design was converted into working hardware with the associated processing procedures developed over a number of months of debugging and testing. This single-unit lamination prototype, sized for manufacturing, was replicated with only minor changes into a double-unit laminator for installation into the Tucson facility. During the debugging period, downtime of this new design was significant. Modifications to the non-reliable hardware are presently being implemented and are expected to resolve this issue, reducing the down time significantly. Figure 3.7 shows a photograph of this double-unit laminator in the Tucson facility.
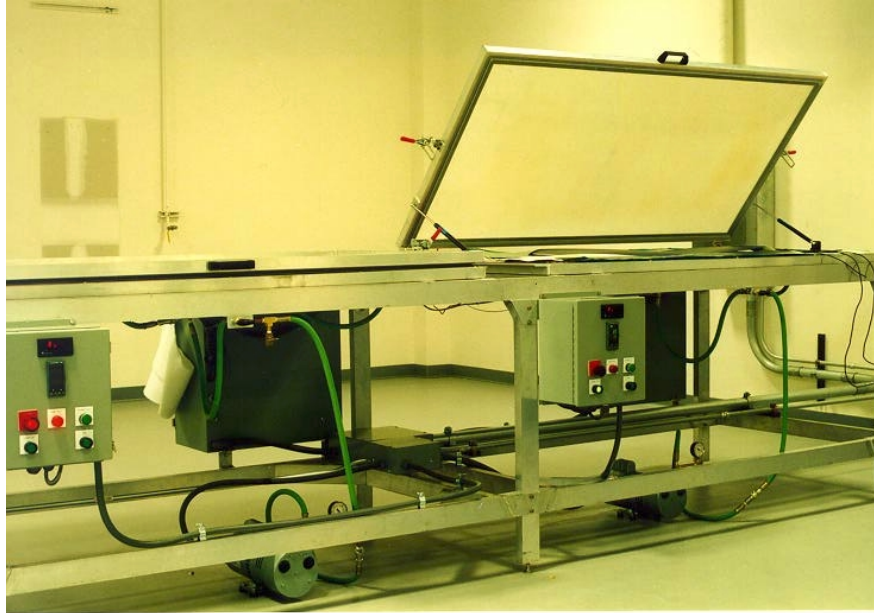


**Figure 3.7.** Photograph of a double-unit, single-bag laminator

It has been determined that manual lay-up of the five layers utilized for flexible products is a labor-intensive process. Automation will likely be necessary to accomplish both the quality and throughput rate goals. In that light, a simple, high-productivity, semi-automated, "Buss-bar and Lay-up Apparatus" has been envisioned. The conceptual design phase of this apparatus has been completed. Significant testing and proving-in of this design will be required to ensure high quality at near 100% yields at throughput rates of 2-4 $ft^2$/minute, but no overwhelming roadblocks are expected. The expected rewards are high in both quality and productivity.

During the next phases of this subcontract, the focus within this subtask will be primarily on the following:

- Further demonstrations of new module designs (flexible, semi-flexible, and rigid) processed through this and other lamination equipment.
- Improved uptime on the existing laminators through relatively minor modifications to existing laminators.

- Resolving, through tests, the remaining engineering design questions on the "buss bar and lay-up apparatus" in order to move forward with implementation of manufacturing equipment.
- Determining a conceptual design for next-generation methods for accomplishing roll-to-roll lay-up and lamination of product.

## 3.3  Lamination of Flexible Substrate to Semi-Flexible Backing

The objective of this subtask is to demonstrate the ability to fabricate modules to backings that are not flexible.  The list of material options here was significant enough that we changed the original term of "rigid" into two categories rather than one.  This separation of "semi-flexible" and "rigid" backing allows us to align our efforts with the needs of the identified markets.  This section describes the primary accomplishments against the objectives within this subtask.

Figure 3.5 shows an unframed module where the backing chosen was aluminum.  Demonstration modules have been made for several of these options, but no stress testing has been accomplished to date to confirm or deny concerns related to delamination at the EVA-metal interface under conditions of high-humidity exposure.

During the next phases of this subcontract, the focus within this subtask will be primarily on the following:

- Demonstration and stress testing of metal-backed, semi-rigid modules,
- Demonstration and stress testing of "rigid" glass-backed product designs.

## 3.4  Power Lead and Buss Attachment

The objective of this subtask is to design, demonstrate, and incorporate parts, materials, and procedures for the range of steps in solar module fabrication from buss bar application to power lead attachment in order to meet initial throughput, economic, and market needs of GSE.  This section describes the primary accomplishments against the objectives within this subtask, separating further into Buss Bars and Lead Termination.

### 3.4.1  Buss Bars

The primary requirement for a buss bar system is to make a low-resistance contact to the metallic electrode on the end cells of a module and to retain those properties over stresses representative of the application environment.

Buss bar tape and conductive inks were selected.  On some of the buss bars, the conductive pastes were applied to evaluate improved contact reliability.  Test dummies were fabricated with the goal of monitoring resistance changes during stressing, and initial stresses were accomplished. Figure 3.8 shows a photograph of a test dummy.  The contact resistance was determined at various points in the test including:

- Before lamination,

- After lamination,
- Before and after mechanical rolling of the dummy over a 3-in. diameter pipe,
- After thermal stressing at 90°C for 1 hour,
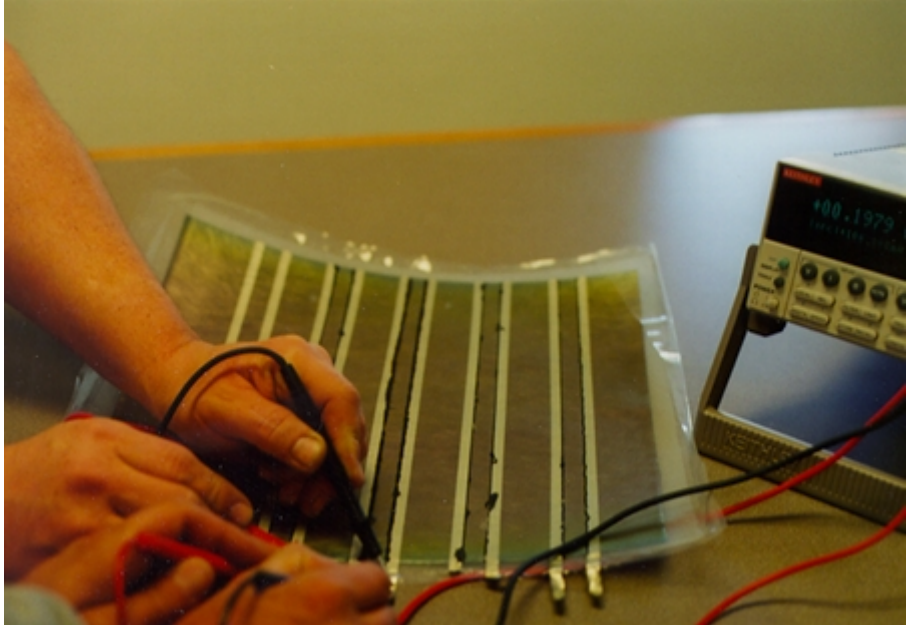- After thermal stressing at 90°C for 24 hours.



**Figure 3.8.**  Test dummy being tested after stressing.

Table 3.1 shows the calculated power losses increase ($I^2R$) due to resistance increase of buss bar contacts for four different chosen materials/configurations.  It is assumed that a reasonable allowable power loss threshold for modules is 0.5%.  The absolute error associated with these values is ~+-0.01%.

**Table 3.1.**  Calculated power losses for buss bar stress tests

| Condition | After Lamination | Before Mechanical Stressing | After Mechanical Stressing | After 1 Hour at 90C | After 24 Hours at 90C |
|---|---|---|---|---|---|
| No Paste | 0 (Baseline) | 0.09% | 0.10% | 0.18% | 0.23% |
| Paste B | 0 (Baseline) | 0.014% | 0.033% | 0.024% | 0.10% |
| Paste C | 0 (Baseline) | 0.14% | 0.19% | 0.26% | 0.66% |

The conclusions of this test are that:
1) For initial, short term stresses, for No Paste and for Paste B, there appears to be no real issue with increases in power loss due to resistance increase of the buss bars or contacts to TCO layer.
2) There are choices of paste that make the effect worse.

3) More stress testing will be accomplished in the next phase.

To ensure that the selected buss bar system remains stable during its life in the field, well designed thermal exposure, humidity exposure, and thermal cycling tests will be accomplished in the next phases of this subcontract. Further testing will utilize not only the best choices from this test but other selections as well.

### 3.4.2 Power Lead Terminations

A simple means has been developed to attach the power leads to the buss bars. The method is made even more straightforward due to the ability to form holes in this polymeric structure without expensive or time-consuming jigs or equipment.

Figure 3.9 shows the parts utilized in the junction box for lead termination.
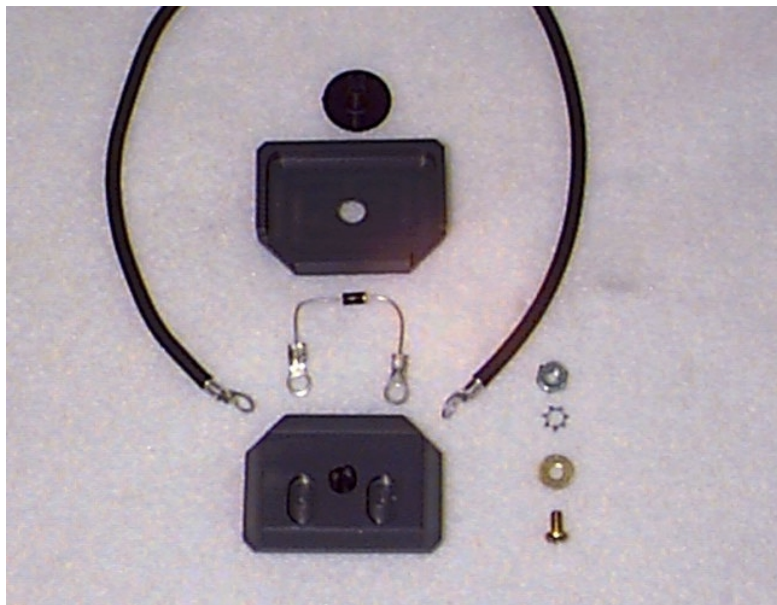


**Figure 3.9.** Parts utilized for lead termination and junction

With multiple products, one challenge is to reduce the number of custom designs required. It is believed that the same lead termination methodology will be utilized on all flexible products. For semi-flexible and rigid products, the mainstream methodology of soldering buss bars to a foil strip attached to the junction box terminal is still considered the best option. Efforts to ensure that such a system remains stable during thermal exposure, humidity exposure, and thermal cycling are yet to be accomplished.

**Summary**

During the first year of effort under this subcontract, a number of significant advancements were made. After numerous iterations, a complete set of effusion sources was successfully demonstrated in the CIGS manufacturing system during Phase I. Another significant accomplishment that occurred was the demonstration of a 9.8% device from CIGS deposited on polyimide in a roll-coater. The compatibility of GSE processes for CdS and the TCO depositions was continuously verified as improvements in the absorber deposition process were made. In addition, the groundwork for further efficiency increases was laid by initiating a program to incorporate Na into roll-coated CIGS films.

A program to explore deposition of CIGS films on stainless steel substrates was also initiated. A preliminary result was the demonstration of an 8.4% efficient device from CIGS roll-coated onto a stainless steel substrate.

Significant delays were encountered in acquiring the equipment required for monolithic integration, but rapid progress in process development was made once the equipment was facilitated at GSE. Many aspects of the back contact, via, and front contact scribes have been verified by electrical and microscopic techniques. The ink dispense technology, an integral part of the interconnect scheme, has demonstrated continuous ink lines less than 200 μm wide, comparable to good screen-printing, but with a much better registration accuracy.

The GSE product line was redefined, and demonstrations of laminated active modules were accomplished at the GSE facility. Materials and module layouts for initial GSE products were resolved. Appropriate suppliers of critical materials were identified that meet the initial cost goals for GSE initial product lines. Product demonstrations of several of the initial GSE products have been made, and such demonstrations continue.

Equipment to accomplish rapid lamination throughputs of product at low costs for all initially envisioned product lines was identified and procured. Two laminators are now installed, mostly debugged, and fully operational. Total throughputs for the two existing laminators has been standardized at a maximum rate of ~60ft$^2$/hour. A conceptual design for a "buss bar and lay-up apparatus" was completed and that equipment, once incorporated, is expected to result in significant increases in productivity and quality in manufacturing. First-generation methods for lead termination (buss bar to lead connection) were identified, demonstrated, and are now incorporated into the "standard" process. Preliminary investigation of the materials utilized was initiated by Underwriters Laboratory (UL) experts to pave the way toward product certification of the GSE products.

**Future Plans**

Moving into Phase II, greater emphasis will be placed on the improving the yield and reproducibility of the CIGS deposition process rather than on increasing the maximum efficiency of small area test cells. Determining the tolerance of the process with respect to changes in the CIGS deposition parameters is the first task that will be accomplished. The incorporation of Na into the CIGS films will be more fully explored with the yield issue continually in mind. The

effect of any changes will be evaluated in the context of complete module fabrication, including window layers, monolithic integration, and encapsulation. Work on stainless steel substrates will be accelerated to the point that test modules will be generated early in Phase II.

To differing degrees, all scribing processes require further optimization. The back contact scribe appears to function well electrically; future effort will focus on reducing the width of that scribe and berm.

The front contact scribe, in which the TCO is selectively cut by laser methods, appears to be successful microstructurally but needs to be validated electrically. The front contact scribe will be tested using small area devices and submodules. Front contact scribes made under varying conditions will be used to isolate small area cells. Tests on these small area devices will be then be used to look for complete isolation and shunt formation from front to back contacts. Although presently the width of the front contact scribe is not excessive by usual standards (about 80 microns), we will attempt to change the scribing parameters to further reduce scribe width.

Electrical testing and validation will also be a focus of effort for the interconnect ("via") scribe also. Interconnect test structures will be used to optimize process conditions to produce low resistivity via scribes.

Process development under the ink-jet deposition task will include minimization of the linewidth and improvement in line uniformity. Compatibility with the subsequent TCO process must be assured with no degradation in adhesion or scribe resistivity. Several other types of material will be evaluated, and the process will be extended to larger areas. Typical linewidth of the ink-jet printed insulator, presently about 250 microns, is already better than what we could obtain with screen-printing. Our goal is to further reduce the width by about a factor of two, minimizing lost module area.

Future work under the lamination task will focus primarily on further equipment improvements, process development, product demonstrations and stress testing. In particular, further demonstrations of new module designs (flexible, semi-flexible, and rigid) will be performed with existing and improved lamination equipment. Improved uptime on the existing laminators will be made through relatively minor modifications to existing laminators. Stress testing of all three module types will also be initiated.

Tests will be conducted to resolve the remaining engineering design questions on the "buss bar and lay-up apparatus" in order to move forward with implementation of manufacturing equipment. A conceptual design for next-generation methods for accomplishing roll-to-roll lay-up and lamination of product will also be determined. To ensure that the selected buss bar system and power lead terminations remain stable during its life in the field, well designed thermal exposure, humidity exposure, and thermal cycling tests will be accomplished in the next phases of this subcontract.

## References

[1]      S. Wiedeman, R.G. Wendt, J.S. Britt, "Module Interconnects on Flexible Substrates", NCPV Photovoltaics Program Review; Proceedings of the 15th Conference, Denver, CO, 1998; AIP Conference Proceedings (in press).

## Acknowledgements

# REPORT DOCUMENTATION PAGE

| 1. AGENCY USE ONLY (Leave blank) | 2. REPORT DATE<br>September 1999 | 3. REPORT TYPE AND DATES COVERED<br>Phase I Technical Report, 5 February 1998 – 4 February 1999 |
|---|---|---|

**4. TITLE AND SUBTITLE**
Process Development for CIGS-Based Thin-Film Photovoltaic Modules; Phase I Technical Report, 5 February 1998 – 4 February 1999

**6. AUTHOR(S)**
J. Britt, S. Wiedeman, R. Wendt, and S. Albright

**5. FUNDING NUMBERS**

C: ZAK-8-17619-04
TA: PV905001

**7. PERFORMING ORGANIZATION NAME(S) AND ADDRESS(ES)**
Global Solar Energy, L.L.C.
5575 South Houghton Road
Tucson, AZ  85747

**8. PERFORMING ORGANIZATION REPORT NUMBER**

**9. SPONSORING/MONITORING AGENCY NAME(S) AND ADDRESS(ES)**
National Renewable Energy Laboratory
1617 Cole Blvd.
Golden, CO  80401-3393

**10. SPONSORING/MONITORING AGENCY REPORT NUMBER**

SR-520-26840

**11. SUPPLEMENTARY NOTES**

NREL Technical Monitor: H.S. Ullal

**12a. DISTRIBUTION/AVAILABILITY STATEMENT**
National Technical Information Service
U.S. Department of Commerce
5285 Port Royal Road
Springfield, VA 22161

**12b. DISTRIBUTION CODE**

**13. ABSTRACT** *(Maximum 200 words)*
This report describes work performed by Global Solar Energy (GSE) under Phase I of this subcontract. GSE has initiated an extensive and systematic plan to accelerate the commercialization of thin-film photovoltaics (PV) on copper indium gallium diselenide (CIGS). GSE is developing the technology to deposit and monolithically integrate CIGS photovoltaics on a flexible substrate. CIGS-deposited on flexible substrates can be fabricated into either flexible or rigid modules. Low-cost, rigid PV panels for remote power, bulk/utility, telecommunications, and rooftop applications will be produced by affixing the flexible CIGS to an expensive rigid panel by lamination or adhesive. In the GSE approach, long (up to 700 m) continuous rolls of substrate are processed, as opposed to individual small glass plates. In combination with roll-to-roll processing, GSE is developing evaporation deposition operations that enable low-cost and high-efficiency CIGS modules. Efforts are under way to transition the CIGS deposition process into manufacturing at GSE. CIGS process development is focused on synchronizing the operation of the effusion sources, the Se delivery profile, substrate temperature, and a host of other parameters. GSE has selected an interconnect scheme and procured, installed, and tested the equipment necessary to implement the cell interconnection for thin-film CIGS modules on a polyimide substrate.

**14. SUBJECT TERMS**

photovoltaics ; copper indium gallium diselenide ; CIGS ; roll-to-roll vacuum deposition ; CIGS deposition ; low-cost PV panels ; high-efficiency modules ; flexible polyimide substrate

**15. NUMBER OF PAGES**

**16. PRICE CODE**

| 17. SECURITY CLASSIFICATION OF REPORT<br>Unclassified | 18. SECURITY CLASSIFICATION OF THIS PAGE<br>Unclassified | 19. SECURITY CLASSIFICATION OF ABSTRACT<br>Unclassified | 20. LIMITATION OF ABSTRACT<br>UL |
|---|---|---|---|